

## RESEARCH ARTICLE

# Effects of Zinc Oxide Nanoparticles on Pyruvate Dehydrogenase and Lactate Dehydrogenase Expressions and Apoptotic Index in Breast Cancer Cells

Cem ÖZİÇ<sup>1,†</sup>  Barış YILDIZ<sup>2,†</sup>  Ramazan DEMİREL<sup>3</sup>  Özkan ÖZDEN<sup>4</sup> 

† These authors contributed equally to this study

<sup>1</sup> Kafkas University, School of Medicine Department of Medical Biology, TR-36100 Kars - TÜRKİYE<sup>2</sup> Kafkas University, Institute of Health Sciences Department of Physiology, TR-36100 Kars - TÜRKİYE<sup>3</sup> Kafkas University, Institute of Natural and Applied Sciences Department of Biotechnology, TR-36100 Kars - TÜRKİYE<sup>4</sup> Kafkas University, Faculty of Engineering and Architecture Department of Bioengineering, TR-36100 Kars - TÜRKİYE(\*) **Corresponding author:** Cem ÖZİÇ and Özkan ÖZDENCellular phone: +90 532 272 78 91 (C. Öziç),  
+90 536 564 52 29 (Ö. Özden)E-mail: oziccem@gmail.com (C. Öziç),  
ozzkan1@gmail.com (Ö. Özden)

How to cite this article?

**Öziç C, Yıldız B, Demirel R, Özden Ö:**Effects of zinc oxide nanoparticles on pyruvate dehydrogenase and lactate dehydrogenase expressions and apoptotic index in breast cancer cells. *Kafkas Univ Vet Fak Derg*, 30 (4): 489-496, 2024.  
DOI: 10.9775/kvfd.2024.31688

Article ID: KVFD-2024-31688

Received: 29.01.2024

Accepted: 15.06.2024

Published Online: 25.06.2024

## Abstract

Zinc oxide nanoparticles (ZnO-NPs) are metal oxide NPs that have high cytotoxicity on cancer cells and low cytotoxicity on healthy cells. Breast cancer is the most frequent type of cancer-causing death among women worldwide. In this study, anti-cancer effects of ZnO-NPs were investigated. For this purpose, we treated the MCF7 and MDA-MB-231 breast cancer cell lines and human umbilical vein endothelial cells HUVEC cell line with 10 µg/mL and 20 µg/mL ZnO-NP. Anti-cancer effects of ZnO-NPs were evaluated with cell viability, apoptotic index and colony formation assays, and anti-Warburg effect were investigated by evaluating of pyruvate dehydrogenase (PDH) and Lactate Dehydrogenase A (LDHA) protein expressions. Results indicated that, ZnO-NP application did not have a cytotoxic effect on HUVEC cells, it had cytotoxicity on both breast cancer cell lines. However, MCF7 cells were more sensitive to ZnO-NP treatment. Administration of 20 µg/mL ZnO-NP reduced the survival of MCF7 cells by 62% and increased the apoptotic index by approximately 6 times. Additionally, ZnO-NP treatment inhibited the doubling times of cells and suppressed the colony-forming abilities of both breast cancer cell lines. Also, it was seen that ZnO-NP treatment increased PDH expression in MCF7 cells, where the apoptotic index was more induced. As a result, we have shown for the first time that ZnO-NPs affect the energy metabolism of cells by increasing PDH expression in MCF7 cells, thus increasing the apoptotic index. Our study, which observed the anticancer effects of ZnO-NPs on breast cancer cells, will also shed light on future experimental studies.

**Keywords:** Breast cancer, Lactate dehydrogenase A, MDA-MB-231, MCF7, Pyruvate dehydrogenase, Zinc oxide nanoparticles

## INTRODUCTION

Cancer, the second leading cause of death worldwide, is a group of oncological diseases characterized by the irregular growth and proliferation of a single cell by the accumulation of different mutations as a result of impaired cell control. Breast cancer, on the other hand, is a type of cancer with a high prevalence among women <sup>[1]</sup>. There are different subtypes of breast cancer and the pathological classification of these subtypes is evaluated according to the expression of estrogen (ER), progesterone (PR), and human epidermal 2 (HER2) proteins by tumor tissue <sup>[2]</sup>. Breast cancers that do not have ER, PR, and HER2 protein expressions are referred to as triple negative cancer (TNBC), thus they are known

as a more aggressive type for prognosis and curation. On the other hand, breast cancer that expresses hormone receptors is classified as a hormone receptor-positive (HR+) subtype and it has a better prognosis thus it is admitted as a subtype that easily takes under control <sup>[3]</sup>. Conventional treatment methods against breast cancer include radiotherapy, hormonotherapy, chemotherapy, and surgical interventions <sup>[4]</sup>. However, since tumor tissue can show heterogeneous mutation distribution, the bioavailability of conventional treatments is less than expected <sup>[5]</sup>. In this respect, the use of nanoparticles (NP) designed for treatment or diagnosis in the field of nanotechnology is a current area of research <sup>[6]</sup>. Various NPs based on organic, inorganic, lipid, protein, glycan, or



synthetic polymers are used to develop new therapeutic agents for use in cancer treatment. On the other hand, the use of commercially produced NPs in cancer treatments contributes to low toxicity by increasing drug efficacy [7]. In addition, numerous reports show that NPs have a high affinity for reaching specific organelles such as mitochondria and nuclei [8]. It is also known that rationally engineered NPs by modulating particle size, morphology, and surface modifications can also infiltrate hypoxic regions of tumor mass [8,9].

Metal oxide NPs of zinc (Zn), copper (Cu), silver (Ag), and gold (Au) elements are frequently used in various anti-cancer studies [11-14]. Among all these metal oxide NPs, zinc oxide NPs (ZnO-NP) are considered a promising NP compound due to their selective cytotoxic, biocompatible, easily synthesizable and designable characters, as well as exhibiting anti-microbial, anti-bacterial, anti-oxidant activities [15-17]. With many studies, it has been determined that ZnO-NPs affect different oncogenic intracellular signaling pathways and have antiproliferative effects in many cancer types such as colon, breast, lung, oval, cervical, and stomach at low doses [18-21]. On the other hand, another advantage of ZnO-NPs is that they show their cytotoxic effects on healthy cells at high doses [21]. The selective anti-cancer capabilities of ZnO-NPs are generally thought to proceed by triggering different anti-apoptotic proteins by increasing the production of intracellular reactive oxidant species (ROS) [22-24]. ZnO-NP treatment also depletes levels of glutathione (GSH), superoxide dismutase (SOD) and catalase (CAT) enzymes and modulate Bax/Bcl-2 ratio in favor of apoptosis in cancer cells [22]. Also, it was demonstrated that ZnO-NP treatment causes translocation of pro-apoptotic proteins from mitochondria to cytosol [25]. Therefore, one of the main cellular targets of ZnO-NPs is mitochondria, therefore it could be thought that ROS inducing activity of ZnO-NPs must be related with disturbed membrane potential of the mitochondria [22,25].

Enhanced intracellular ROS levels are also indirectly related to cell's energy metabolism, and cancer cells are the cells with disturbed energy metabolism [26]. Cancer cells almost always prefer glycolysis for ATP production because ATP production by oxidative phosphorylation is the main source of intracellular ROS, thus increased amounts of ROS are associated with increased apoptotic stimulus [27]. Therefore, it is conceivable that there may be a mechanistic relation between ZnO-NP and Warburg effect. Evaluation of pyruvate dehydrogenase (PDH) and Lactate dehydrogenase A (LDHA) protein levels are used to test of modulation effects of some candidate modulators on the energy metabolism of cells and enhanced PDH levels are related to enhanced apoptotic stimulation [26-28].

In this study, we aimed to investigate anti-cancer

properties and anti-Warburg effects of ZnO-NPs on two breast adenocarcinoma cell lines and HUVEC cells for toxicity assays. MDA-MB-231 and MCF7 cells were used because these cells represent two different breast cancer phenotypes, respectively triple negative (TNBC) and hormone positive (HR+) subtypes. For this aim, the anti-proliferative, anti-colonial, and apoptosis induction and effects of ZnO-NPs on protein levels of PDH and LDHA were investigated.

## MATERIAL AND METHODS

### Cell Culture

MDA-MB-231 and MCF7 breast adenocarcinoma cell lines (ATCC, USA) and human Umbilical Vein Endothelial Cell (HUVEC) lines (ATCC, USA) were used in the study. Breast cancer cell lines were selected for the different phenotypes they represent; as a TNBC phenotype MDA-MB-231 cell line represent more aggressive and less curable phenotype while MCF7 cell line represent well-curable HR+ phenotype of breast cancer. Cells were cultured in sterile petri dishes with Dulbecco's Modified Eagle Medium (DMEM) (SIGMA, USA) containing 10% fetal bovine serum (FBS) (SIGMA, USA) and 1% antibiotic (Penicillin-Streptomycin) (GIBCO, USA) and incubated in an incubator with a temperature of 37°C, 5% CO<sub>2</sub> and free moisture. All the used cell lines were provided as commercially and an approval of ethical is not necessary.

### Cell Viability Assay

Cells were seeded in sterile 96-well microplates containing  $3 \times 10^3$ /100  $\mu$ L cells in each well (n=6). The seeded cells were incubated under the specified conditions for 48 h, ensuring ~70% reproduction. Concentrations of 10  $\mu$ g/mL and 20  $\mu$ g/mL of ZnO-NP (Nanografi Nano Technology, Türkiye) with a diameter of 30-50 nm were applied to the cells for 24 h, and at the end of the 23<sup>rd</sup> h, 10  $\mu$ L of CVDK-8 Cell Viability Kit (EcoTech, Türkiye) was added to each well. A group that was untreated with ZnO-NP was included in the experiment as the control group in each cell lines. The microplate was incubated at 37°C for 60 min and at the end of the 24<sup>th</sup> h in total, the absorbance values of the samples were obtained by reading at 450 nm via Multiskan SkyHigh Microplate Spectrophotometer (Thermo Scientific, USA). The obtained absorbance values were converted into percentage values using the absorbance values of the control group as 100% and used in statistical analysis.

### Doubling Time

When the cells were planted in a 96-well sterile microplate, the initial absorbance values were obtained. By using the initial absorbance values obtained and the absorbance values of the application groups at the end of the 24<sup>th</sup> h, the

folding times were determined according to the groups. Online Doubling Time Calculator Tool (<http://www.doubling-time.com/compute.php>) was used to determine the folding times for the calculation of folding times.

### Cell Harvesting and Homogenization

Cells seeded in sterile petri dishes were treated with 10 µg/mL and 20 µg/mL ZnO-NP doses and incubated for 24 h. At the end of the time, the media were removed and the cells were washed twice with cold PBS (pH: 7.4) on ice, and the cells were scraped with 2 mL of cold PBS and transferred to Eppendorf tubes. The tubes were centrifuged at 4°C and 1200 rpm for 5 min, and pellets were obtained by removing supernatants. Pellets were lysed by a freeze-thaw method using lysis buffer (TNN + NP40 + PMSF). Total protein amounts were determined using the Bradford Protein Assay Kit II kit (Biorad, USA) at a wavelength of 595 nm.

### Western Blotting

Samples were standardized to forty µg of protein and subjected to 10% Tris-Glycine-sodium dodecyl sulfate-polyacrylamide gel electrophoresis. Blotting was carried out using polyvinylidene difluoride membranes (PVDF). The membranes were incubated overnight at 4°C with anti-pyruvate dehydrogenase (PDH) (Cell Signaling, USA), anti-lactate dehydrogenase (LDHA) (Cell Signaling, USA) and anti-β-actin (Santa Cruz, USA) primary antibodies. After three washes, the membranes were incubated with horseradish peroxidase (HRP)-conjugated secondary antibody (Abcam, UK) at room temperature for 30 min. Subsequently, the membranes were washed, and images were captured following treatment with the enhanced chemiluminescence substrate (ECL) (Biorad, USA).

### Colony Formation Assay

Cells were seeded in a sterile 6-well plate containing 200 cells in each well (n=6) and incubated for 48 h. At the end of the period, the cells were treated with 10 µg/mL and 20 µg/mL ZnO-NP and the experiment was continued for 14 days. Also, a group that was untreated with ZnO-NP was included in the experiment as a control group in each cell lines. At the end of the experimental period, the medium was removed, and the wells were washed with PBS (pH: 7.4). After washing, the cells were fixed with fixative buffer (1 acetic acid: 7 ethanol). Following the procedure, the colonies were stained with crystal violet. The plates were placed in a water tank to remove crystal violet remains and the plates were left to dry overnight. The drying plates were photographed, and the colonies were converted into numerical data by using the Analyze Particle Tool in the ImageJ 1.53m program and used in statistical analysis<sup>[31]</sup>. Colonies containing fewer than 50 cells were not included in the calculation.

### Acridine Orange (AO) and Ethidium Bromide (EB) Staining

Cells were seeded in sterile plates with 24 wells at a density of  $1.5 \times 10^3$ /mL and incubated for 48 h. At the end of the period, the cells were incubated for 24 h with doses of 10 µg/mL and 20 µg/mL ZnO-NP. Also, ZnO-NP untreated groups were considered as control group for each cell lines. After incubation, each well was washed with PBS (pH: 7.4) and stained with a solution containing 100 µg/mL AO and EB. Cell images were photographed via a fluorescence microscope (EVOS FL, Invitrogen) and images taken from red and green channels were merged. For statistical analysis, 200 cells were counted in each group and classified as live, dead, and apoptotic.

### Statistical Analyses

Microsoft Excel 365 and IBM SPSS 26.0 were used to perform statistical analyses. Shapiro-Wilk normality test and Levene homogeneity test were applied to the results. A one-Way ANOVA test was applied to the parameters in line with the significance values obtained and the Games-Howell PostHoc test was used for pairwise comparisons. Frequencies evaluated with Pearson Chi-Square ( $\chi^2$ ) test. All quantitative analyses were repeated six times. Results were considered statistically significant at  $P < 0.05$ .

## RESULTS

### ZnO-NP is Cytotoxic on Breast Cell Lines but Not on HUVEC Cell Line

The effects of 10 µg/mL and 20 µg/mL ZnO-NP treatments in MDA-MB-231, MCF7, and HUVEC cell lines on the survival at the end of 24 h were shown in *Fig. 1*. The results showed that ZnO-NPs have a cytotoxic effect on both cancer cell lines. It was determined that both treatment doses significantly reduced cell survival compared to the control group ( $P < 0.001$ ) in MDA-MB-231 cells. However, there was no statistically significant difference between these two dose groups in MDA-MB-231 cells. However, a dramatic decrease in cell survival was observed in the group treated with 20 µg/mL ZnO-NP ( $P < 0.001$ ) in MCF7 cells, while no cytotoxic effect was observed in the 10 µg/mL ZnO-NP treated group. On the other hand, no cytotoxic inhibition in cell survival was observed in HUVEC cells for both ZnO-NP treated groups (*Fig. 1-B*).

### Periods of Doubling Times of Breast Cancer Cells Increase with ZnO-NP Treatment

*Fig. 2* illustrates the impact on the cell doubling times of MDA-MB-231 and MCF7 breast cancer cell lines following the application of 10 µg/mL and 20 µg/mL ZnO-NPs for 24 h. Findings from the doubling times showed that 10

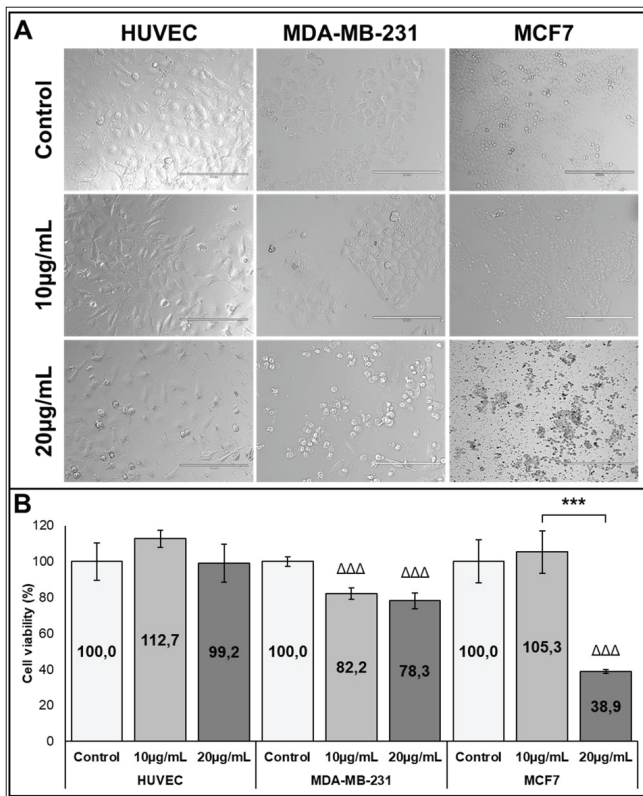


Fig 1. The effects of 10 µg/mL and 20 µg/mL ZnO-NPs doses applied for 24 h on cell survival of MDA-MB-231 and MCF7 breast adenocarcinoma cancer cells and HUVEC non-cancerous cells are shown in A (calibration bar=200 µm). The numerical data obtained by converting the absorbances obtained as a result of measurements with the CVDK-8 Cell Viability kit into percentages compared to the control groups and the statistical analysis results are shown in B. The delta (Δ) symbol indicates the statistical difference between the relevant groups compared to the control group, and the star symbol (\*) indicates the statistical difference between the specified groups. (ΔΔΔ, \*\*\*P<0.001)

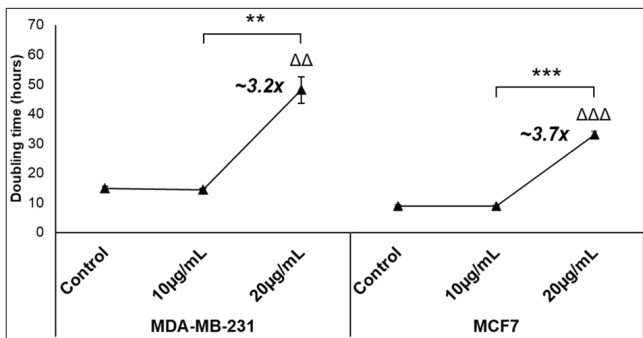


Fig 2. Effect of 10 µg/mL and 20 µg/mL ZnO-NPs doses applied to MDA-MB-231 and MCF7 breast adenocarcinoma cancer cell lines for 24 h on cell doubling times. The delta (Δ) symbol indicates the statistical difference of the relevant groups compared to the control group, and the star symbol (\*) indicates the statistical difference between the specified groups. (ΔΔ, \*\*P<0.01, ΔΔΔ, \*\*\*P<0.001)

µg/mL ZnO-NP administration had no effect on cell folds, but 20 µg/mL ZnO-NP administration increased the folding times by ~3.2 times (P<0.01) in MDA-MB-231 cells and ~3.7 times (P<0.001) in MCF7 cells.

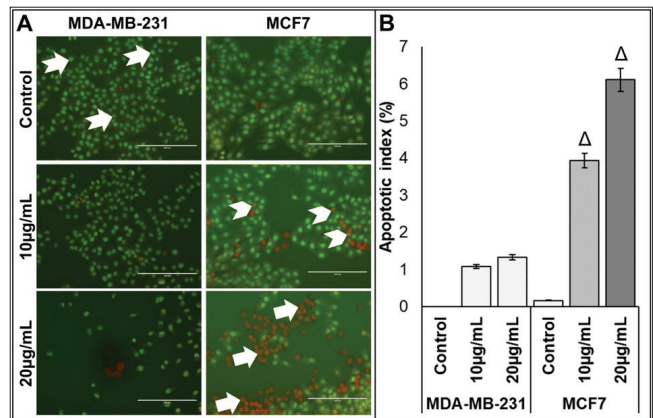


Fig 3. Effects of 10 µg/mL, 20 µg/mL ZnO-NPs doses applied to MDA-MB-231 and MCF7 breast adenocarcinoma cancer cell lines for 24 h on apoptosis, effects by fluorescence microscopy and acridine orange (AO)/ethidium bromide (EB) staining, panel A' is also shown (calibration bar = 200 µm). Cut arrows with a head indicate live cells; cut arrows with no head indicate apoptotic cells; uncut arrows with a head indicate dead cells. Chi-Square (χ<sup>2</sup>) statistics test results of apoptotic and dead cell formations are also shown in B (Δ<sup>2</sup>P<0.05)

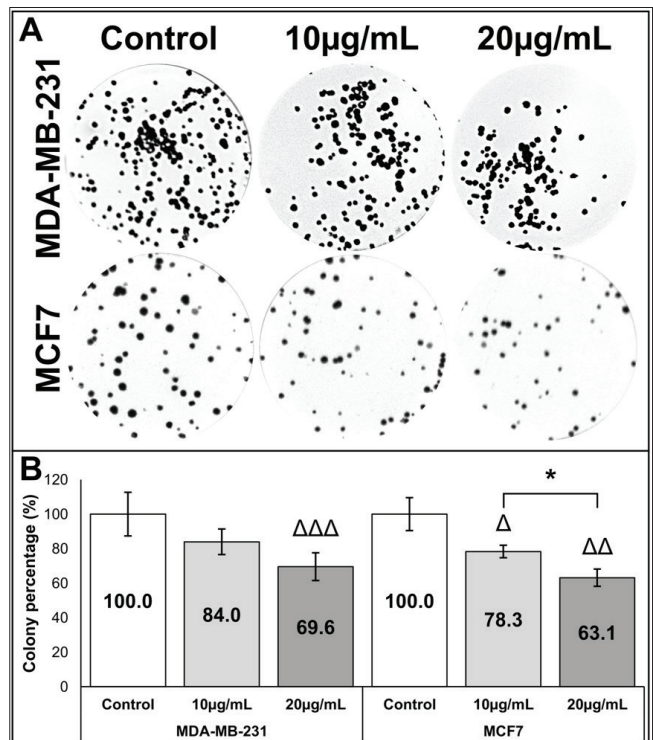


Fig 4. The effects of 10 µg/mL and 20 µg/mL ZnO-NPs doses applied for 14 days on colony formation of MDA-MB-231 and MCF7 breast cancer cells are shown in A. Statistical differences obtained by converting colony numbers into percentage values are shown in B. The delta (Δ) symbol indicates the statistical difference of the relevant groups compared to the control group, and the star symbol (\*) indicates the statistical difference between the specified groups (ΔΔΔ, \*\*\*P<0.001)

### ZnO-NP Treatment Induces Apoptotic Index in MCF7 Cell Line

AO stains the nuclei of the living cell green, while EB only stains cells that have lost their membrane integrity

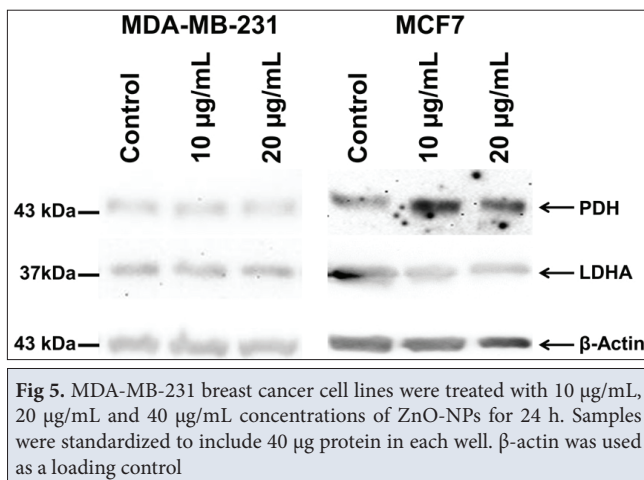


Fig 5. MDA-MB-231 breast cancer cell lines were treated with 10 µg/mL, 20 µg/mL and 40 µg/mL concentrations of ZnO-NPs for 24 h. Samples were standardized to include 40 µg protein in each well.  $\beta$ -actin was used as a loading control

red. For this reason, living cells appear in green, dead cells appear in red, and apoptotic cells appear in orange [32]. Merged AO (green) and EB (red) fluorescent images of both breast cell lines after ZnO-NP treatments for 24 h were shown in Fig. 3-A, and frequencies of the apoptotic cells were shown in the graph in Fig. 3-B. It was observed that apoptotic formation did not induce in MDA-MB-231 cells treated with ZnO-NP. On the other hand, 10 µg/mL ZnO-NP treatment increased apoptotic index up to ~4 times and 20 µg/mL ZnO-NP treatment increased up to ~6 times ( $P < 0.05$ ) in MCF7 cells.

#### Treatment of ZnO-NP Suppresses Colony Forming Ability of MDA-MB-231 and MCF7 Cell Lines

The colony percentages of MDA-MB-231 and MCF7 breast cancer cells treated with ZnO-NP doses at the end of 14 days were shown in Fig. 4-A. 10 µg/mL ZnO-NP treatment reduced colony numbers about ~16% in MDA-MB-231 cells and ~22% in MCF7 cells ( $P < 0.05$ ) when compared with the control groups. MDA-MB-231 cells exhibited a reduction of ~31% in their colony-forming abilities compared to the control group when treated with 20 µg/mL ZnO-NP ( $P < 0.001$ ). Similarly, MCF7 cells showed suppression of ~37% ( $P < 0.01$ ) under the same conditions (Fig. 4-B).

#### PDH Protein Expression of MCF7 Cells is Enhanced with ZnO-NP Treatment

Expression changes in PDH and LDHA proteins of MCF7 and MDA-MB-231 cells after 24 h of ZnO-NP treatment were shown in Fig. 5.  $\beta$ -actin antibody was used as a loading control. Results indicate that neither 10 µg/mL nor 20 µg/mL of ZnO-NP treatment did not affect PDH and LDHA protein expressions in MDA-MB-231 cells. On the other hand, PDH expression of MCF7 cells after ZnO-NP treatments was found as enhanced but LDHA expression was not affected. However, there was no expression difference between 10 µg/mL and 20 µg/mL ZnO-NP treatment groups.

## DISCUSSION

ZnO-NPs are metal oxide nanoparticles that selectively induce cell death in cancer cells [33]. ZnO-NPs have been supported by *in vivo* and *in vitro* studies that show several biological effects that can cause cell toxicity, including cytotoxicity, and also inhibit cell proliferation [24,34-36]. Studies have shown that ZnO-NPs have cytotoxic effects on a large cancer cell spectrum such as HepG-2, MCF-7, HeLa, U87, and S91 cells [37]. Similarly, our results show that ZnO-NPs are cytotoxic to MCF7 and MDA-MB-231 breast cancer cells, but MCF7 cells are more sensitive to ZnO-NP treatment. On the other hand, it is known that ZnO-NPs are used in photodynamic therapy methods and as drug transporters due to their low cytotoxicity and targeted selective properties [38-41]. Our findings also show that cytotoxic doses of ZnO-NPs on MCF7 and MDA-MB-231 breast cancer cells do not cause cytotoxic effects on umbilical endothelial HUVEC cells.

The experimental effects of ZnO-NPs are not limited just to *in vitro* studies, there are some promising *in vivo* results for the treatment of cancer. It was shown that ZnO-NP synergistically increased the effectiveness of anti-cancer drugs by inducing apoptosis *in vivo* conditions by Nabil et al. [42]. The disruption of the balance between apoptosis and proliferation in cells is also an important element of carcinogenesis. Therefore, activating apoptotic pathways is a useful anti-cancer strategy. ZnO-NPs are also thought to induce apoptosis by affecting pro-apoptotic proteins in mitochondria, which play key roles in inducing apoptosis [33,43]. The data obtained in this study show that 20 µg/mL dose application to MCF7 cells, which are more sensitive to ZnO-NP treatment, increases the apoptotic index up to 6 times. However, we did not observe the same effect in MDA-MB-231 breast cancer cells. We think that the difference between these two breast cancer cells may be related to the different breast cancer phenotypes (TNBC and HR+) that these cells represent.

Colony formation is the ability of a cell to multiply and form a colony under the stress of division, which is suppressed when left alone. Most of the cancer cells originate from only a single cell and they can metastasize and invade to distant tissues or nearby tissues. Therefore, an effective anti-cancer agent is also expected to suppress the colony-forming ability of cancer cells [44]. NPs are also suppressor agents on the colony-forming ability of cancer cells [24,45]. Our findings also show that ZnO-NPs suppress the long-term colony formation ability of MCF7 and MDA-MB-231 breast cancer cells. However, the dose of ZnO-NP (20 µg/mL), which suppresses cell viability more effectively in MCF7 cells compared to MDA-MB-231 cells, does not show inhibition in the same proportion of its effect on colony formation of MCF7 cells. We think

that this may be related to the rate of degradation of the NP structure in the medium or the resistance developed by cancer cells to cytotoxic ZnO-NP stress in the long term.

Changes in the expression of many proteins in cancer cells cause some conditions. Cancer cells convert pyruvate to lactate, which is formed as a result of glycolysis via Warburg effect. This process gives less energy than glycolysis while providing rapid energy production in cancer cells [46]. For this reason, modulating energy metabolism in cancer cells is a useful anti-cancer strategy. There is some evidence indicating that NPs suppress the Warburg effect. It was demonstrated that AuNPs reduce glycolysis by suppressing the activity of Glucose transporter 1 (GLUT1) and Hexokinase 2 (HK2) enzymes [47]. On the other hand, another study shows that suppressing the Warburg effect via an NP-mediated manner is dependent on induced ROS in osteosarcoma Saos-2 cells [48]. These findings indicate that NPs affect cellular ROS metabolism and cause apoptotic formation. In the present study, we also examined PDH and LDHA protein expression in ZnO-NP-treated breast cancer cell lines MCF7 and MDA-MB-231. LDHA and PDH proteins are two proteins that are closely related to the Warburg effect due to their key role in the balance between glycolysis and oxidative phosphorylation in cancer cells. Our results indicate that ZnO-NP treatment causes an increase in PDH expression but not in LDHA expression in MCF7 cells which represent the HR+ breast cancer subtype however we did not find the same results in MDA-MB-231 cells which represent the TNBC subtype. There are considerable amounts of previous reports indicating that inhibition of PDH is related to promoted apoptotic stimulation [28,29,49]. Therefore, as expected, ZnO-NP-treated MCF7 cells were the groups in which apoptosis was the most promoted in our study. Also, according to a previous report, zinc facilitates the transport of pyruvate into mitochondria and is closely associated with cellular energy status [50]. Therefore, the regulation of PDH by ZnO-NP is not surprising and needs further mechanistic studies and more cancer models to determine the relation at molecular level.

As a result, it was observed that ZnO-NP inhibited cell viability in MCF7 and MDA-MB-231 breast cancer cell lines with no toxic effects in healthy cells. Also, the ability of colony formation of both cell lines was suppressed thanks to ZnO-NP treatment. Correspondingly, the duplication time of both breast cancer cells was found prolonged. However, ZnO-NPs were more cytotoxic on MCF7 cells and increased the apoptotic index more when compared to MDA-MB-231 cells. On the other hand, we determined an enhanced pattern in PDH expression of ZnO-NPs treated MCF7 cells, which was the most apoptotic stimulation determined. Since the

increased activity of PDH is associated with increased apoptotic stimulation, we think that the anti-cancer properties of ZnO-NPs in MCF7 cells lie in the activating effects of PDH. For this reason, ZnO-NP is thought to have the potential to inhibit the growth of cancer cells. However, the apoptotic mechanism induced by ZnO-NP appears to induce different results on mutant metabolic elements between MCF7 cell lines representing the HR+ breast cancer phenotype and MDA-MB-231 cell lines representing the TNBC phenotype. Therefore, we think that further studies should elucidate the apoptotic pathway targets of ZnO-NPs in breast cancer cells representing HR+ and TNBC phenotypes.

## DECLARATIONS

**Availability of Data and Materials:** All data are presented in the manuscript.

**Acknowledgments:** We are grateful to Cansu Beytur and Süphan Özçağdavul from Kafkas University for their supports in the laboratory assays.

**Financial Support:** This work was supported by the Research Fund of the Kafkas University with 2021-TS-85 project number.

**Ethical Statement:** This study does not require ethics committee approval.

**Conflict of Interest:** The authors declared that there is no conflict of interest.

**Author Contributions:** Study design/planning: CÖ, BY, ÖÖ. Data collection/entry: BY, CB, SÖ, RD. Data analysis/statistics: CÖ, BY, TA, ÖÖ. Data interpretation: CÖ, BY, ÖÖ. Preparation of manuscript: CÖ, BY, TA, ÖÖ. Literature analysis/ search: CÖ, BY, ÖÖ.

## REFERENCES

1. Divya M, Govindarajan M, Karthikeyan S, Preetham E, Alharbi NS, Kadaikunnan S, Khaled JM, Almanaa TN, Vaseeharan B: Antibiofilm and anticancer potential of  $\beta$ -glucan-binding protein-encrusted zinc oxide nanoparticles. *Microb Pathog*, 141:103992, 2020. DOI: 10.1016/j.micpath.2020.103992
2. Keenan TE, Tolaney SM: Role of immunotherapy in triple-negative breast cancer. *J Natl Compr Canc Netw*, 18, 479-489, 2020. DOI: 10.6004/jncn.2020.7554
3. Cardoso F, Kyriakides S, Ohno S, Penault-Llorca F, Poortmans P, Rubio IT, Zackrisson S, Senkus E, ESMO Guidelines Committee: Early breast cancer: ESMO Clinical Practice Guidelines for diagnosis, treatment and follow-up†. *Ann Oncol*, 30, 1194-1220, 2019. DOI: 10.1093/annonc/mdz173
4. Smalley KSM, Herlyn M: Towards the targeted therapy of melanoma. *Mini Rev Med Chem*, 6, 387-393, 2006. DOI: 10.2174/138955706776361402
5. Langer R: Drug delivery and targeting. *Nature*, 392 (6679 Suppl.): 5-10, 1998.
6. McNeil SE: Nanoparticle therapeutics: A personal perspective. *Wiley Interdiscip Rev Nanomed Nanobiotechnol*, 1, 264-271, 2009. DOI: 10.1002/wnan.6
7. Bellusci M, La Barbera A, Padella F, Mancuso M, Pasquo A, Grollino MG, Leter G, Nardi E, Cremisini C, Giardullo P, Pacchierotti F: Biodistribution and acute toxicity of a nanofluid containing manganese iron oxide nanoparticles produced by a mechanochemical process. *Int J Nanomedicine*, 9, 1919-1929, 2014. DOI: 10.2147/IJN.S56394

8. Wang H, Li J, Wang Y, Gong X, Xu X, Wang J, Li Y, Sha X, Zhang Z: Nanoparticles-mediated reoxygenation strategy relieves tumor hypoxia for enhanced cancer therapy. *J Control Release*, 319, 25-45, 2020. DOI: 10.1016/j.jconrel.2019.12.028
9. Liu CG, Han YH, Kankala RK, Wang SB, Chen AZ: Subcellular performance of nanoparticles in cancer therapy. *Int J Nanomedicine*, 15, 675-704, 2020. DOI: 10.2147/IJN.S226186
10. Karmous I, Pandey A, Haj KB, Chaoui A: Efficiency of the green synthesized nanoparticles in cancer therapy: Insights on plant-based bioengineered nanoparticles, biophysical properties, and anticancer roles. *Biol Trace Elem Res*, 196, 330-342, 2020. DOI: 10.1007/s12011-019-01895-0
11. Maliki M, Ifijen IH, Ikhuoria EU, Jonathan EM, Onaiwu GE, Archibong UD, Ighodaro A: Copper nanoparticles and their oxides: optical, anticancer and antibacterial properties. *Int Nano Lett*, 12, 379-398, 2022. DOI: 10.1007/s40089-022-00380-2
12. Rahimi KSMG, Seyedi SMR, Karimi E, Homayouni-Tabrizi M: The cytotoxic properties of zinc oxide nanoparticles on the rat liver and spleen, and its anticancer impacts on human liver cancer cell lines. *J Biochem Mol Toxicol*, 33:e22324, 2019. DOI: 10.1002/jbt.22324
13. Zhang H, Li T, Luo W, Peng GX, Xiong J: Green synthesis of Ag nanoparticles from *Leucis aspera* and its application in anticancer activity against alveolar cancer. *J Exp Nanosci*, 17, 47-60, 2022. DOI: 10.1080/17458080.2021.2007886
14. Faizan M, Bhat JA, Chen C, Alyemeni MN, Wijaya L, Ahmad P, Yu F: Zinc oxide nanoparticles (ZnO-NPs) induce salt tolerance by improving the antioxidant system and photosynthetic machinery in tomato. *Plant Physiol Biochem*, 161, 122-130, 2021. DOI: 10.1016/j.plaphy.2021.02.002
15. Lone MI, He Z, Stoffella PJ, Yang X: Phytoremediation of heavy metal polluted soils and water: Progresses and perspectives. *J Zhejiang Univ Sci B*, 9, 210-220, 2008. DOI: 10.1631/jzus.B0710633
16. Martinez CR, Joshi P, Vera JL, Ramirez-Vick JE, Perales O, Singh SP: Cytotoxic studies of PEG functionalized ZnO nanoparticles on MCF-7 cancer cells. In, NSTI Nanotechnol. Conf. Expo, NSTI-nanotech, 2011.
17. Bai DP, Zhang XF, Zhang GL, Huang YF, Gurunathan S: Zinc oxide nanoparticles induce apoptosis and autophagy in human ovarian cancer cells. *Int J Nanomedicine*, 12, 6521-6535, 2017. DOI: 10.2147/IJN.S140071
18. Bai K-J, Chuang KJ, Ma CM, Chang TY, Chuang HC: Human lung adenocarcinoma cells with an EGFR mutation are sensitive to non-autophagic cell death induced by zinc oxide and aluminium-doped zinc oxide nanoparticles. *J Toxicol Sci*, 42, 437-444, 2017. DOI: 10.2131/jts.42.437
19. De Angelis I, Barone F, Zijno A, Bizzarri L, Russo MT, Pozzi R, Franchini F, Giudetti G, Uboldi C, Ponti J, Rossi F, De Berardis B: Comparative study of ZnO and TiO<sub>2</sub> nanoparticles: physicochemical characterisation and toxicological effects on human colon carcinoma cells. *Nanotoxicology*, 7, 1361-1372, 2013. DOI: 10.3109/17435390.2012.741724
20. Dhivya R, Ranjani J, Bowen PK, Rajendhran J, Mayandi J, Annaraj J: Biocompatible curcumin loaded PMMA-PEG/ZnO nanocomposite induce apoptosis and cytotoxicity in human gastric cancer cells. *Mater Sci Eng C*, 80, 59-68, 2017. DOI: 10.1016/j.msec.2017.05.128
21. Ostrovsky S, Kazimirsky G, Gedanken A, Brodie C: Selective cytotoxic effect of ZnO nanoparticles on glioma cells. *Nano Res*, 2:882-890, 2009. DOI: 10.1007/s12274-009-9089-5
22. Akhtar MJ, Ahamed M, Kumar S, Khan MM, Ahmad J, Alrokayan SA: Zinc oxide nanoparticles selectively induce apoptosis in human cancer cells through reactive oxygen species. *Int J Nanomedicine*, 7, 845-857, 2012. DOI: 10.2147/IJN.S29129
23. Choudhury SR, Ordaz J, Lo C-L, Damayanti NP, Zhou F, Irudayaraj J: From the cover: Zinc oxide nanoparticles-induced reactive oxygen species promotes multimodal cyto- and epigenetic toxicity. *Toxicol Sci*, 156, 261-274, 2017. DOI: 10.1093/toxsci/kfw252
24. Vimala DS, Murugesan R, Francesco M, Antara B, Xiao FS, Surajit P: Comparative study on anti-proliferative potentials of zinc oxide and aluminium oxide nanoparticles in colon cancer cells. *Acta Biomed*, 90, 241-247, 2019. DOI: 10.23750/abm.v90i2.6939
25. Li Z, Guo D, Yin X, Ding S, Shen M, Zhang R, Wang Y, Xu R: Zinc oxide nanoparticles induce human multiple myeloma cell death via reactive oxygen species and Cyt-C/Apaf-1/Caspase-9/Caspase-3 signaling pathway *in vitro*. *Biomed Pharmacother*, 122:109712, 2020. DOI: 10.1016/j.biopha.2019.109712
26. Chen X-S, Li L-Y, Guan Y, Yang J-M, Cheng Y: Anticancer strategies based on the metabolic profile of tumor cells: Therapeutic targeting of the Warburg effect. *Acta Pharmacol Sin*, 37, 1013-1019, 2016. DOI: 10.1038/aps.2016.47
27. Ghanbari Movahed Z, Rastegari-Pouyani M, Mohammadi MH, Mansouri K: Cancer cells change their glucose metabolism to overcome increased ROS: One step from cancer cell to cancer stem cell? *Biomed Pharmacother*, 112:108690, 2019. DOI: 10.1016/j.biopha.2019.108690
28. Ozden O, Park S-H, Wagner BA, Song HY, Zhu Y, Vassilopoulos A, Jung B, Buettner GR, Gius D: SIRT3 deacetylates and increases pyruvate dehydrogenase activity in cancer cells. *Free Radic Biol Med*, 76, 163-172, 2014. DOI: 10.1016/j.freeradbiomed.2014.08.001
29. Sun J, Li J, Guo Z, Sun L, Juan C, Zhou Y, Gu H, Yu Y, Hu Q, Kan Q, Yu Z: Overexpression of pyruvate dehydrogenase E1 $\alpha$  subunit inhibits warburg effect and induces cell apoptosis through mitochondria-mediated pathway in hepatocellular carcinoma. *Oncol Res*, 27, 407-414, 2019. DOI: 10.3727/096504018X15180451872087
30. Xu L, Li Y, Zhou L, Dorfman RG, Liu L, Cai R, Jiang C, Tang D, Wang Y, Zou X, Wang L, Zhang M: SIRT3 elicited an anti-Warburg effect through HIF1 $\alpha$ /PDK1/PDHA1 to inhibit cholangiocarcinoma tumorigenesis. *Cancer Med*, 8, 2380-2391, 2019. DOI: 10.1002/cam4.2089
31. Rueden CT, Schindelin J, Hiner MC, DeZonia BE, Walter AE, Arena ET, Eliceiri KW: ImageJ2: ImageJ for the next generation of scientific image data. *BMC Bioinformatics*, 18:529, 2017. DOI: 10.1186/s12859-017-1934-z
32. Ribble D, Goldstein NB, Norris DA, Shellman YG: A simple technique for quantifying apoptosis in 96-well plates. *BMC Biotechnol*, 5:12, 2005. DOI: 10.1186/1472-6750-5-12
33. Wahab R, Siddiqui MA, Saquib Q, Dwivedi S, Ahmad J, Musarrat J, Al-Khedhairi AA, Shin HS: ZnO nanoparticles induced oxidative stress and apoptosis in HepG2 and MCF-7 cancer cells and their antibacterial activity. *Colloids Surf B Biointerfaces*, 117, 267-276, 2014. DOI: 10.1016/j.colsurfb.2014.02.038
34. Aoulthana WM, Omar NI, El-Feky AM, Hasan EA, Ibrahim NE-S, Youssef AM: *In vitro* study on effect of zinc oxide nanoparticles on the biological activities of *Croton tiglium* L. seeds extracts. *Asian Pac J Cancer Prev*, 23, 2671-2686, 2022. DOI: 10.31557/APJCP.2022.23.8.2671
35. Kollur SP, Prasad SK, Pradeep S, Veerapur R, Patil SS, Amachawadi RG, S RP, Lamraoui G, Al-Kheraif AA, Elgorban AM, Syed A, Shivamallu C: Luteolin-fabricated ZnO nanostructures showed PLK-1 mediated anti-breast cancer activity. *Biomolecules*, 11:385, 2021. DOI: 10.3390/biom11030385
36. Tas A, Keklikcioglu Cakmak N, Agbektas T, Silig Y: Cytotoxic activity of zinc oxide/titanium dioxide nanoparticles on prostate cancer cells. *IJCT*, 3, 113-120, 2019. DOI: 10.32571/ijct.613536
37. Roshini A, Jagadeesan S, Cho Y-J, Lim J-H, Choi KH: Synthesis and evaluation of the cytotoxic and anti-proliferative properties of ZnO quantum dots against MCF-7 and MDA-MB-231 human breast cancer cells. *Mater Sci Eng C Mater Biol Appl*, 81, 551-560, 2017. DOI: 10.1016/j.msec.2017.08.014
38. Kishwar S, Asif MH, Nur O, Willander M, Larsson PO: Intracellular ZnO nanorods conjugated with protoporphyrin for local mediated photochemistry and efficient treatment of single cancer cell. *Nanoscale Res Lett*, 5, 1669-1674, 2010. DOI: 10.1007/s11671-010-9693-z
39. Mitra S, B S, Patra P, Chandra S, Debnath N, Das S, Banerjee R, Kundu SC, Pramanik P, Goswami A: Porous ZnO nanorod for targeted delivery of doxorubicin: *In vitro* and *in vivo* response for therapeutic applications. *J Mater Chem*, 22, 24145-24154, 2012. DOI: 10.1039/C2JM35013K
40. Shandiz SAS, Sharifian F, Behboodi S, Ghodrathpour F, Baghbani-Arani F: Evaluation of metastasis suppressor genes expression and *in vitro* anti-cancer effects of zinc oxide nanoparticles in human breast cancer cell lines MCF-7 and T47D. *Avicenna J Med Biotechnol*, 13, 9-14, 2021. DOI: 10.18502/ajmb.v13i1.4576

41. Zhang Q, Pan Y, Ma X, Yang H, Chang J, Hong L, Yan H, Zhang S: Elevated secretion of aldosterone increases TG/HDL-C ratio and potentiates the Ox-LDL-induced dysfunction of HUVEC. *Cell J*, 23, 61-69, 2021. DOI: 10.22074/cellj.2021.7033
42. Nabil A, Elshemy MM, Asem M, Abdel-Motaal M, Gomaa HF, Zahran F, Uto K, Ebara M: Zinc oxide nanoparticle synergizes sorafenib anticancer efficacy with minimizing its cytotoxicity. *Oxid Med Cell Longev*, 2020:1362104, 2020. DOI: 10.1155/2020/1362104
43. Boskabadi SH, Balanezhad SZ, Neamati A, Tabrizi MH: The green-synthesized zinc oxide nanoparticle as a novel natural apoptosis inducer in human breast (MCF7 and MDA-MB231) and colon (HT-29) cancer cells. *Inorg Nano-Met Chem*, 51, 733-743, 2020. DOI: 10.1080/24701556.2020.1808991
44. Franken NAP, Rodermond HM, Stap J, Haveman J, van Bree C: Clonogenic assay of cells *in vitro*. *Nat Protoc*, 1, 2315-2319, 2006. DOI: 10.1038/nprot.2006.339
45. Aventaggiato M, Preziosi A, Cheraghi Bidsorkhi H, Schifano E, Vespa S, Mardente S, Zicari A, Uccelletti D, Mancini P, Lotti LV, Sarto MS, Tafani M: ZnO nanorods create a hypoxic state with induction of HIF-1 and EPAS1, autophagy, and mitophagy in cancer and non-cancer cells. *Int J Mol Sci*, 24:6971, 2023. DOI: 10.3390/ijms24086971
46. Urbańska K, Orzechowski A: Unappreciated role of LDHA and LDHB to control apoptosis and autophagy in tumor cells. *IJMS*, 20:2085, 2019. DOI: 10.3390/ijms20092085
47. Sun L, Liu Y, Yang N, Ye X, Liu Z, Wu J, Zhou M, Zhong W, Cao M, Zhang J, Mequanint K, Xing M, Liao W: Gold nanoparticles inhibit tumor growth via targeting the Warburg effect in a c-Myc-dependent way. *Acta Biomater*, 158, 583-598, 2023. DOI: 10.1016/j.actbio.2022.12.054
48. Yang Y, Tao B, Gong Y, Chen R, Yang W, Lin C, Chen M, Qin L, Jia Y, Cai K: Functionalization of Ti substrate with pH-responsive naringin-ZnO nanoparticles for the reconstruction of large bony after osteosarcoma resection. *J Biomed Mater Res A*, 108, 2190-2205, 2020. DOI: 10.1002/jbm.a.36977
49. Chen X, Hao B, Li D, Reiter RJ, Bai Y, Abay B, Chen G, Lin S, Zheng T, Ren Y, Xu X, Li M, Fan L: Melatonin inhibits lung cancer development by reversing the Warburg effect via stimulating the SIRT3/PDH axis. *J Pineal Res*, 71:e12755, 2021. DOI: 10.1111/jpi.12755
50. Yang X, Wang H, Huang C, He X, Xu W, Luo Y, Huang K: Zinc enhances the cellular energy supply to improve cell motility and restore impaired energetic metabolism in a toxic environment induced by OTA. *Sci Rep*, 7:14669, 2017. DOI: 10.1038/s41598-017-14868-x